Fearghal O'Connor

POROUS SILICON-BASED SENSOR TO DETECT BIOFILM GROWTH

MASTER'S DEGREE THESIS

Supervised by Dr. Beatriz Prieto Simón

MASTER'S DEGREE IN NANOSCIENCE, MATERIALS AND PROCESSES

UNIVERSITAT ROVIRA I VIRGILI

Tarragona 2022

Keywords- Porous silicon, biofilm sensor, electrochemical sensor, *S. epidermis.*

Abstract

Bacteria preferentially exist in a sessile or biofilm state which is implicated directly or indirectly in numerous issues across a wide variety of industries and sectors. Once mature, biofilms are very difficult to remove and due to their properties are resistant to chemical and physical stresses. The biofilm formation process is a complex and sequential one. Such complexity might be one of the reasons why there is a lack of identified early indicators of biofilm formation and available early detection methods. Conventional methods to detect biofilms rely on destructive techniques with relatively long turnaround times on obtaining results. This is unsuitable for certain fields such as in the clinic where early intervention has a favourable impact on whether a treatment is successful or not. Here we describe the fabrication process of porous silicon (pSi) substrates, with different surface modifications, that are able to act as an electrochemical sensing platform, and investigate their suitability as substrates for biofilm growth. First, biofilm growth conditions were optimized and biofilms were optically characterized. Among the various types of carbon-stabilized pSi samples, thermally hydrocarbonized pSi (THCpSi) showed the highest biomass through crystal violet staining, and bacterial viability via a LIVE/DEAD fluorescence test. Nonetheless, all carbon-stabilized pSi samples showed high non-specific adsorption of dyes, which was confirmed by Fourier-transform Infrared Spectroscopy. Finally, cyclic voltammetry was used to check the feasibility to electrochemically assess biofilm formation. Results using THCpSi as biofilm substrate and electrode simultaneously underpinned the potential of electrochemically detecting biofilm formation

INTRODUCTION

Bacterial biofilm

Biofilms are complex three-dimensional architectural communities of microorganisms formed by one or more species that are either bound to a surface or encapsulated in a self-made extracellular matrix (ECM) of extracellular polymeric substances (EPSs): proteins, carbohydrates and lipids [1]. Prokaryotes (e.g. bacteria and Archae) and Eukaryotes (e.g yeast) can form biofilm.

Biofilms (particularly, bacterial) can form on any surface (biotic or abiotic) and even on surface to air interfaces. They often form as a response to harsh environmental conditions and thus their properties offer protection to the inhabiting microbes from chemical and physical stress. Consequently, this makes biofilms difficult to remove, causing problems for a wide variety of industries and fields. The food, water distribution, energy harvesting and navel industries among others are all negatively impacted by biofilms.

However, in the medical field, the immediate and often strongest impact of biofilms on human health and wellbeing is obvious. Approximately 80% of infections are attributed to biofilms. They also form on the surface of medical devices, leading to device failure and grave infections. Biofilms also promote and allow for microbial colonization of the exposed tissue which delays or prevents wound healing.

Bacteria exist in nature in two states: planktonic and sessile. The sessile state of bacteria is their immobile state where they have typically attached to a surface and can form biofilm. The majority of bacteria exist in this state [2]. Biofilm formation is a dynamic and complex physiological process that involves the following five main steps in all bacteria species:

1. Reversible attachment
2. Irreversible attachment/ early development of the biofilm
3. Maturation of the biofilm
4. Cell density is reached
5. Dispersion of bacteria into the planktonic state

1.Reversible attachment

Bacteria can colonize biotic (e.g. epithelial cells of the gastrointestinal tract) or abiotic (e.g. glass) surfaces. Bacteria such as *Escherichia coli (E. coli)* have a tail-like appendage called a flagellum that allows for active mobility and chemotaxis to overcome the repulsive forces that exist in an aqueous environment that would otherwise inhibit or reduce adhesion or contact with a surface [3], [4]. For both commensal and pathogenic bacteria, initial adhesion is the first step towards the colonization of a surface [5].

2.Irreversible attachment/ Early development of biofilm

Upon initial attachment, the bacteria become sessile and the expression for the flagellum is repressed thus reducing their active mobility [3], [6]. When culturing bacteria specifically for biofilm formation, the detection of the flagellum indicates that biofilm has not formed. An increased concentration of small molecules, such as cyclic-diguanylic acid (c-di-GMP), can indicate the shift from the planktonic to the sessile state. The concentration of c-di-GMP has been shown to rise in *E. coli* when they transition to the sessile state [7]. Extracellular adhesion organelles, such as type 1 fimbriae and curli fimbriae, are important for the irreversible attachment of bacteria to both biotic and abiotic surfaces. Initial adhesion of many Gram-negative bacteria promotes type 1 fimbriae expression. These adhesion organelles are implicated in the pathogenesis of Urinary Tract Infections (UTIs) by binding to mannose-containing receptors on the epithelium of the urethra[8]. Curli fimbriae, produced by several species of enteric pathogens, are required for both cell-to-surface and cell-to-cell adhesion. They are present in *E. coli* to allow their attachment to both biotic and abiotic surfaces.

3.Maturation of biofilm

The adherent cells start to secrete EPSs which consist of proteins, lipids, nucleic acids and polysaccharides that encase the microorganisms in a matrix and allow them to aggregate facilitating gene transfer and other cell-to-cell communications. These EPSs go someway into explaining how a biofilm protects the resident microbes from the host environment by providing a physical barrier. The EPSs also assist in adherence and the trapping of nutrients that can be subsequently consumed by the microbes present.

Cell-to-cell communications are regulated by autoinducers which regulate and induce the expression of biofilm specific genes.

4.Cell density reached

In this stage, the biofilm becomes a multi-layered 3D structure with compartments that are separated by water channels which function to deliver nutrients to the microbes and remove any toxins produced [8]. Despite these water channels, as the biofilm matures and the population density increases, nutrients can become scarce and toxic metabolites can accumulate driving the need for the next phase of biofilm formation: the dispersion of bacteria.

5.Dispersion of bacteria

Here the bacteria on the superficial layers of the now matured biofilm return to their motile, planktonic state which allows them to leave the original location and spread to other areas of the surface or host organism. In this phase, the genes for the expression of the flagellum (returning motility) and saccharolytic enzymes that digest the EPS biofilm are upregulated, and help free the bacteria from the matrix [1]. Once the dispersed bacteria encounter a new surface, the process of returning to their sessile state to produce a biofilm starts again.

Advantages of biofilm formation (for the residents)

As mentioned above, the formation of biofilm offers multiple advantages to the residing microorganisms and can often be formed as a defensive mechanism to create a more favorable environment for growth and survival of microbes like bacteria [9]. The secreted matrix itself is also a surface that promotes the adhesion of other bacteria to the biofilm.

Bacteria can also engage in a type of symbiosis called syntrophism or syntrophy whereby metabolically different distinct species of bacteria depend on each other for the utilization of their specific energy sources, and a biofilm provides the optimal environment for syntrophism to occur [9]. For example, the degradation of complex organic material involves the coordination of three types of bacteria. First, a fermentation species initiates the process and produces acids and alcohols. These compounds are in turn metabolized by an acetogenic species. Finally, a methanogen extracts energy from the metabolized compounds and forms methane [10].

Impact on industries

The water distribution, energy and navel industries are all affected negatively by the formation of bacterial biofilms. Bacterial adhesion and biofilm formation directly lead and exacerbate biofouling which is the accumulation of biological matter and organisms onto a wetted surface. Biofouling accelerates corrosion on metallic and concrete surfaces and is responsible for 40% and 20% of the corrosion in gas and oil pipelines, respectively, increasing maintenance costs and the risk of safety incidents [11]. It also causes significant economic losses in the transport and storage of these fuels annually. This is related to the issues that biofilm causes for the navel industry which not only increases the corrosion of ships hulls, but also reduces the speed and fuel efficiency of the vessels.

In drinking water distribution systems (DWDS), biofilms allow colonization of the internal water contacting surfaces and cause multiple problems including corrosion of the pipes, changing the taste and odour of the water, and also potentially being a source of pathogen contamination. Water cooling systems that are used in multiple industries are also subject to the negative consequences on biofilm growth whereby the circulating water flow is compromised, and thus the heat transfer is reduced. Bacteria can enter the system from the water source used and, due to the ideal environmental conditions, their proliferation can occur.

Modern food processing methods provide a favourable environment for biofilm formation on the surfaces of the raw materials being processed. Pathogenic bacteria can be housed in the biofilms formed and thus cause issues for the end users.

In the medical field biofilms have a huge impact economically and, more importantly, on human health and wellbeing. Biofilms can form on any indwelling device and have been observed on prosthetic heart valves, central venous catheters, urinary catheters, titanium joint replacement implants, contact lenses, and intrauterine devices [12]–[14].

Additionally, bacterial biofilms have a key role in the development of antibiotic resistance. Antibiotic resistance is one of the major global challenges that occurs when pathogenic microbes, mainly bacteria, become resistant to treatment compounds. This has huge consequences in the clinic as treatments can be delayed, costs and hospital stays are increased and can even lead to patients' mortality. A number of factors are involved in the development of antibiotic resistance, including over prescription of antibiotics, increased global travel and antibiotic residues in food and water supply. Interestingly, biofilm plays an important role in its development. The physical structure of the biofilm provides bacteria protection by limiting the interactions between bacterial cells and the antimicrobial compound which can bind EPS and be neutralized. The environment inside the EPS also promotes horizontal gene transfer, which is the primary factor in the development of antibiotic resistance. This is where genetic information can be passed from one bacterium to another without the need for an offspring to be generated. Resistance conferring genes can be passed between the bacterial cells of a colony. This makes sessile bacteria 700 times more resistant to antibiotics when compared to their planktonic states [15].

Detecting biofilms

Due to the huge economical and societal impact bacterial biofilms might have on various industries, as well as on our health, their early detection is needed. Biofilm detection has received an increasing amount of attention, particularly in clinical settings where an early diagnosis could potentially improve treatment outcomes and reduce the dosages of antibiotics needed. Numerous techniques have been reported for biofilm detection and characterization in laboratory settings, but many of these are not suitable for real life scenarios.

Biofilm biomarkers

Added to biofilm-related genes as biomarkers of biofilm presence, specific molecules released by the biofilm producing bacteria have been identified as good biomarkers of biofilm formation. Some examples include α-defensin, biofilm-associated protein (BAP) and various peptides and other molecules that make up the biofilm matrix (e.g. cellulose). However, their presence or absence depends on both the location within the biofilm, and the species of the bacteria causing the biofilm [16], [17].

Molecular methods to detect biofilm-related genes

Polymerase Chain Reaction (PCR) can be used to analyze biofilms by detecting the presence of biofilm-related genes. Multiplexed PCR tests can also be designed to detect genes of interest, such as antimicrobial resistant genes. However,

there is a limit to the characteristic information of the bacteria that can be obtained here such as the viability of the cells and whether bacteria are in the sessile or planktonic state. Real world samples (e.g. clinical) may also be contaminated by DNA from other organisms present in the environment, thus affecting the accuracy of these tests [16].

Analytical methods to quantify biofilm biomarkers

Among the various techniques used to detect biofilm biomarkers other than genes, Raman spectroscopy has been often used as it can detect very low concentrations of taxonomical biomarkers and signaling molecules by identifying their unique 'spectral fingerprints'. This can be enhanced by Surface-Enhanced Raman Scattering (SERS) combined with metallic nanoparticles as reported by Nguyen et al., where they were able to detect biofilm formation by *Pseudomonas aeruginosa* (*P. aeruginosa*) by using plasmonic nanosphere probes for the pyocyanin molecule that is implicacted in biofilm formation by that species [18].

Imaging biofilms

Various imaging technologies have been employed in the characterization of biofilms. Confocal microscopy techniques can provide information on the viability, species present and spatial characteristics. However, samples require staining, and these are destructive techniques [19]. Similarly, electron microscopy can provide a lot of useful information, but it is also destructive and requires a clear line of site to the sample so it is not suitable for *in situ* analysis [17].

In order to 'see' biofilm without the need for an invasive procedure, imaging technologies that use near-infrared spectroscopy to clinically image biofilm through bodily tissues have been developed and commercialized. However, this method requires the use of luminescent labels and is dependent on an absence of contra-indications in the patient and risk-to-benefit analysis [17].

Acoustic methods to detect biofilm presence

A novel approach to detecting biofilm is by using Surface Acoustic Waves (SAW) and Love Waves (LW) that are able to distinguish hard material and soft material (i.e. biofilm). While in a controlled laboratory setting this method can detect very early biofilms and provide real-time monitoring of the biofilm formation, more research is needed to determine whether this can be translated into a real-world environment [17].

Electrochemical methods to detect and monitor biofilm formationVarious electrochemical methods have been reported in the literature as both biofilm detection and real-time monitoring techniques. [20][20]

Cyclic voltammetry (CV) involves a redox rection taking place on the working electrode (WE). The potential alternates back and forth through the electrode while the current- potential is measured to plot a characteristic cyclic voltammogram. Becerro et al. were able to detect the early stages of bacterial growth as soon as 1 h after initial culturing of *Staphylococcus epidermis (S. epidermis)* biofilms with CV measurements in growth media [11]. Bacterial cells express a variety of electrochemically active molecules during different phases of attachments and biofilm formation. CV was used to detect the changes in the electrode environment during bacterial culture and biofilm formation. They also carried out differential pulse voltammetry (DPV) measurements to complement the CV results[11]. DPV uses multiple input pulses of current and the output signal is determined by the difference in currents in the before and after applying the pulse. Results showed peaks that correlated with the log, lag and stationary/death phases of bacterial growth, showing potential to be used as a real-time sensor.

Square Wave Voltammetry (SWV) is a type of staircase voltammetry where a current is pulsed between a working and reference electrodes. Measurements are taken at the end of the forward and reverse potential pulses and the differential current waveform is derived by calculating the difference between the two. Belin et al. used SWV to detect metabolically active phenazine compounds which are produced by *P. aeruginosa* at various stages of their growth. Using SWV to characterise specific molecules that are associated with specific physiological states offers a novel approach to detecting metabolically active molecules implicated in the growth of biofilm[21].

Finally, electrochemical impedance spectroscopy (EIS) has some key characteristics that support its potential for real-time monitoring. EIS is a non-destructive technique that can be implemented when biofilm grows on a WE by measuring changes in both resistance and capacitance at the biofilm-electrode interface. Lie et al. demonstrated that both *Salmonella* and *E. coli* biofilms could not only be detected but also distinguished from each other when grown on fabricated electrodes and EIS measurements taken[20]. The capacitance and resistance of the biofilms showed time-

dependent trends that were unique to both species grown which is promising for the development for a sensor providing real-time information[20].[17]

Project Aims

We aim to develop new electrochemical methodologies that can monitor biofilm growth in real time and be used to test the response of the cultured bacteria to antibiotics. To that purpose, this project explores the use of electrochemical sensors to detect and monitor bacterial biofilm growth. Particular attention is given to the design of the sensing platform, as this is where the biofilm will be grown on. Materials such as porous silicon (pSi) are ideal candidates to fabricate sensors due to their large surface area and the possibility to fine tune both their morphological features and surface chemistry. Moreover, pSi has been recently reported to be an excellent choice to design electrochemical sensing platforms, as it can be easily modified to perform as electrochemical transducer.

Therefore, pSi has been chosen as a substrate for this phase of the project due to its morphological and chemical versatility. PSi is prepared via electrochemical anodization of silicon in a hydrofluoric acid solution. The size of the pores, film thickness and surface chemistry can be easily tuned to optimize bacterial biofilm growth and sensor performance. Here we present the fabrication and modification of pSi to deliver three types of electrodes, and demonstrate their use as substrates to grow *S. epidermis* biofilms on their surface. We then compare the optical characterization of the biofilms grown on those pSi substrates, with some preliminary results from their electrochemical characterization via cyclic voltammetry.

MATERIALS AND METHODS

Porous Silicon Electrode Fabrication

PSi electrodes were fabricated via electrochemical anodization of silicon in an HF solution, and then carbon-stabilized through two different methods. On the one hand, pSi samples were stabilized through thermal treatment in the presence of acetylene. Depending on the temperature set for the carbonization step, two types of samples were prepared, namely, thermally hydrocarbonized pSi (THCpSi), and thermally carbonized pSi (TCpSi). On the other hand, pSi was also carbon-stabilized via spin coating a solution of furfuryl alcohol onto the pSi surface, and then proceeding with polymerization and thermal carbonization of the polymeric film (PFApSi).

A 2 cm^2 piece of silicon was cut from a boron doped (p++ type) siliconwafer (Siltronix) with 0.00055–0.001 Ω cm resistivity. These silicon pieces were then cleaned by sonication while submerged in isopropanol (Sigma-Aldrich). The samples were then rinsed in absolute ethanol (Scharlab) and dried using N_2 gas.

The anodization cell was set up by using cylindrical Teflon pieces which are resistant to HF. A Pt electrode acted as the cathode and the silicon wafer acted as the anode. Aluminium foil was used to improve the electrical contact and an O ring was used to ensure the solution was retained inside the cell during the reactions.

First, the silicon pieces were anodically etched under a current density of 350 mA cm^{-2} for 30 s in a 1:1 solution of 48% HF (Merck Millipore) and absolute ethanol (Sigma-Aldrich) to produce a sacrificial layer. To remove this sacrificial layer, the etching solution was removed and 5 M NaOH (Sigma-Aldrich) was added to the cell and left for 5 min. Then, the NaOH was removed, the cell was rinsed with absolute ethanol and dried with N_2 gas to ensure no NaOH residues remained. The second etch was carried out for 100 s in a 3:1 solution of 48% HF and absolute ethanol with a current density of 85 mA cm^{-2} being applied. Again, the etching solution was removed and the cell and sample were rinsed with absolute ethanol before being dried by N_2. The samples were kept in an inert environment while waiting for the next steps. These fabrication steps were identical for all the pSi samples (i.e. TCpSi, THCpSi and PFApSi) to be prepared.

Samples were then carbonized to both stabilize and improve electrical conductivity. This was done in a Carbolite Gero tube furnace with quartz tubes that were only used for each conformation. To prepare THCpSi, prior to carbonization, the quartz tube with the sample in place was purged with N_2 gas for 45 min at room temperature. Then, a 1:1 N_2-acetylene mixture flow was set for 17 min at room temperature before the temperature was ramped at 15 °C/min to 525 °C and held for 15 min. The tube was then allowed to cool to room temperature before the samples were removed. To prepare TCpSi, a 2-step process was followed, in which the first step corresponds to the preparation of THCpSi. Secondly, a 1:1

mix of N_2-acetylene was flown for 10 min at room temperature, followed by annealing at 800°C for 10 min only under N_2 flow. The samples were let cool to room temperature under a N_2 flow before being removed.

To prepare PFApSi, a furfuryl alcohol solution (Sigma-Aldrich) was applied to the surface of the freshly etched pSi via spin coating using a Laurell Model WS-400B spin coater. The solution was prepared using 25 mg of oxalic acid (Sigma Aldrich), 4 mL of ethanol (PanReac) and 1 mL of neat furfuryl alcohol. 250 µL of the FA solution was dispensed onto each pSi sample and was first spun at 700 rpm for 2 min to ensure that the solution had penetrated into the pores. Then the sample was spun at 4000 rpm for 1 min to complete the coating. After spin coating, the samples were placed in the furnace for 2 h at 100°C under an N_2 gas flow to first polymerize the furfuryl alcohol into polyfurfuryl alcohol (PFA). Then for carbonization the temperature was ramped to 700°C for 2h 20 min, again in an N_2 environment. Samples were left cool to room temperature under a N_2 flow before being removed.

Porous silicon characterization

Morphological characterization: Field Emission Scanning Electron Microscopy (FESEM) (Quanta 600 FEI Company) was used to characterize pSi prior to and after biofilm growth. FESEM was used to determine pSi's pore size and film thickness. FESEM was also used to visualize the bacterial cells in the biofilm grown on the pSi electrode surface. Prior to analysis, the biofilm was gold sputtered (Quorum Q150T Plus) to make the surface conductive and thus suitable for SEM analysis.

Chemical characterization: Contact angle measurements were taken to assess wettability and relate changes in wettability with changes in the physicochemical properties of the electrode surface. A drop of water was dropped onto the carbonized pSi surface and a video taken simultaneously by an Ocean Optics camera. The contact angle was measured by OneAtension software and still images of the water droplet on the surface were also obtained.

Electrochemical characterization:

A three-electrode set up with an in-house built three-electrode Teflon cell was used to perform cyclic voltammetry (CV) measurements. The fabricated pSi (THCpSi, TCpSi and PFApSi) as the working electrode (WE), a Ag/AgCl reference electrode and a Pt wire counter electrode were all connected to an Ivium pocketstat potentiostat. Parameters were input into Iviumstat software and the experiments were run. Iviumstat software was also used to analyse the results.

CV measurements were carried out by scanning the applied potential from -0.2 to 0.7 V , at a scan rate of 100 mV/s, using a 2 mM redox species of ferrocyanide and ferricyanide each in a 10 mM PBS buffer as a measuring solution.

Dye/ surface chemistry interactions

In the interest of optimizing the process, the dyes used to characterize biofilm growth and their potential interactions with the pSi surface were investigated. Three dyes were investigated. Crystal Violet stains Gram-positive bacteria as the stain is retained in their thick cell wall. SYTO 9 binds to and stains nucleic acids for both live and dead bacteria giving a green emission. Propidium Iodide is a red-fluorescent dye that is impermeable to cell membranes thus ut stains the DNA of dead (apoptotic) bacteria. Each dye, , was incubated on each one of the three types of carbon-stabilized pSi electrodes and subjected to the protocol steps described below in the biofilm growth section. Samples were sterilized at room temperature in 96% v/v ethanol for 15 min beforehand to ensure that no bacteria were present on the surface susceptible to be subsequently stained.

The pSi samples previously exposed to each dye were then analysed via Fourier Transform Infrared Spectroscopy (FTIR) (JASCO FT/IR-6700) to detect any potential bonds between the dye compounds and each type of carbon-stabilized pSi favoring the non-specific adsorption of the dyes. 32 scans were taken at a resolution of 4.0 cm^{-1} with a range of 4000 – 400 cm^{-1}. The stage was cleaned with acetone and left to dry before each sample was analysed.

Biofilm growth

The bacteria species *S. epidermis* was chosen for this experimental work. *S. epidermis* is a spherical, Gram-positive bacterium that is typically non-pathogenic when found as part of the skin flora. However, it is recognisable for the majority of hospital-acquired infections and can colonise the surfaces of medical devices, especially catheters[22].

Initially culturing protocols required optimization. For crystal violet assays to measure biomass, they were grown on 96-well plates for 24 h, 48 h and 72 h and incubated at a temperature of 37°C. Once the time was optimized, the biofilms were grown on the unetched silicon wafers, stained with viability staining kit and fluorescence images were taken.

Tryptic Soy Broth (TSB) medium was prepared to a concentration as per manufacturer's instructions: 30 g of powder per 1 L of milliQ water. For sterilization the media was then autoclaved for 15 min at 121°C. Pipette tips were also sterilized this way. The biosafety hood was sterilized using Ultraviolet light (UV) for 15 min and was wiped down with alcohol prior to work beginning.

Bacteria samples were first taken from frozen stocks and let thaw at room temperature. 1 mL of stock sample was added to a sterile falcon tube with 9 mL of TSB medium. This solution was then incubated at 37°C for 15 h to increase bacteria cell numbers to a concentration of $2x10^9$ colony forming unit (cfu)/µL . After incubation, the solution was centrifuged at 4000 rpm for 10 min to create a pellet of the bacterial biomass. The pellet was then resuspended in 10 mL of freshly autoclaved TSB medium. The resulting solution was then pipetted onto the fabricated pSi electrode and incubated at 37°C for 24 h for a biofilm to grow.

Biofilm characterization

Bacterial quantification was carried out using crystal violet staining and reading the optical density. A 1% crystal violet solution was prepared using autoclaved milliQ water. Bacterial/biofilm was cultured as above. Each sample was washed three times with 250 µL of physiological saline (0.9% solution of NaCl in milliQ water). 200 µL of 99% methanol was added for fixation of the bacteria and left for 15 min before removing. Samples were then air dried before 200 µL of 1% crystal violet stain was added. This was left for 5 min. Then, the excess/unbound stain was removed by rinsing with tap water. For thorough rinsing the samples were placed in milliQ water and put on an Invitrogen HulaMixer sample mixer for 10 min. This was repeated six times. The samples were then air dried again, but this time under aluminium foil as the crystal violet dye is UV sensitive. 200 µL of 33% glacial acetic acid was added to the samples to dissolve the dye. After 10 min the solution was pipetted into labelled wells on a 96 well plate and then brought to a plate reader (SpectraMax®). Optical density was read at 570 nm.

Bacterial viability was measured using Thermo Scientific LIVE/DEAD® Bac Light Bacterial Viability staining, taking images under fluorescence microscopy and analysing the images using ImageJ software. Biofilm was grown as per the protocol described above. After the final incubation, the samples were placed in the biosafety cabinet and the excess media was removed. 25 µL per sample of SYTO 9 and propidium iodide were mixed in an Eppendorf tube. 25 µL of this solution was added to each sample and left for 15 min. Excess stain was then removed via washing with autoclaved PBS. Fluorescent microscopy was carried out using a Nikon ECLIPSE TE2000-E microscope. The excitation/emission maxima for these dyes used were 480/500 nm for SYTO 9 (live bacteria) stain and 490/635 nm for propidium iodide (dead bacteria).

Electrochemical analysis

CV measurements were carried out in 2 mM ferrocyanide and ferricyanide in a 10 mM PBS buffer solution using pSi samples (THCpSi, TCpSi and PFApSi) as the WE, both pre and post biofilm growth.

RESULTS AND DISCUSSION

PSi characterization

Morphological characterization: FESEM has a greater spatial resolution over conventional SEM and was chosen for morphological characterization of pSi. Although film thickness plays also a role on how pSi favors or hinders biofilm growth, in this study we only focused on pore size.

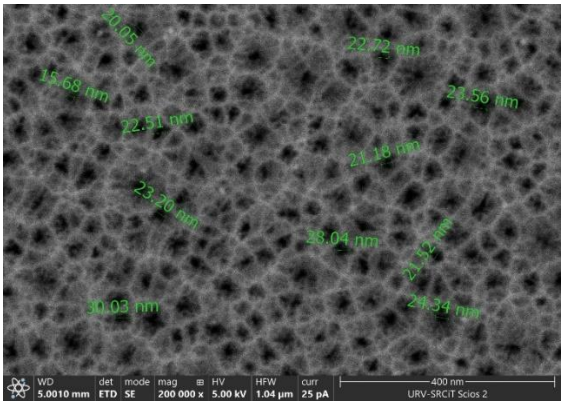

Figure 1: FESEM image of PFApSi sample.

Figure 1 above shows an FESEM image of the surface of a PFApSi sample. For TCpSi and THCpSi the average pore size was found to be between 35-40 nm, and for PFApSi, as shown in Figure 1, the average was found to be 19 nm ± 4 nm. Although all samples were fabricated following the same etching conditions and thus all showed the same pore size upon being freshly etched, the difference in the carbonization method led to the differences observed in the average pore diameter. The smaller pore size observed in the PFApSi sample was indeed expected as this method relies on the polymerization of the infiltrated monomeric solution, which ends up in polymeric coatings of different thicknesses depending on the spin-coating conditions used, and its subsequent carbonization.

Wettability: Contact angle measurements were taken in triplicate. Contact angle values for TCpSi, THCpSi and PFApSi were 37°, 92° and 59°, respectively (Figure 2). THCpSi was confirmed to be hydrophobic while both TCpSi and PFApSi are hydrophilic. These results agree with previous reports, confirming the three carbonization protocols worked well [23].

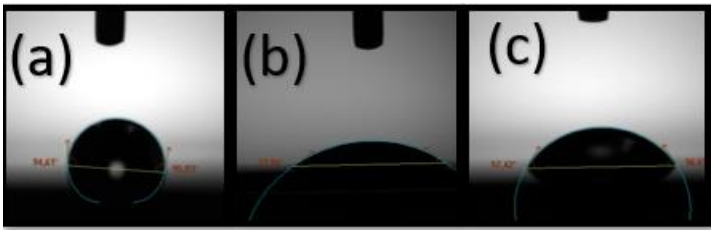

Figure 2: Images of the contact angles of (a) THCpSi, (b) TCpSi and (c) PFApSi.

Electrochemical characterization

CV measurements were performed on all carbon-stabilized pSi samples as explained above. Table 1 summarizes the results.

XXXX To demonstrate the feasibility of using THCpSi, TCpSi and PFApSi, key parameters from the cyclic voltammograms obtained when measuring in a 2 mM $[Fe(CN)_6]^{3-/4-}$ prepared in 10 mM PBS at pH 7.4, need to be assessed. Those parameters include the oxidation and reduction potentials (Epa and Epc) and current intensity (Ipa and Ipc) values for the redox species used, as well as the peak-to-peak potential separation (ΔE).

Table 1: CV characterization. Epa, Epc, Ipa, Ipc and ΔE values using THCpSi, TCpSi and PFApSi as WE. 2 mM ferrocyanide and ferricyanide $[Fe(CN_6)]^{3-/4-}$ prepared in 10 mM PBS buffer, pH 7.4, used as a measuring solution.

Type of carbon-stabilized pSi	***Epa (V)***	***Epc (V)***	***Ipa (µA)***	***Ipc (µA)***	***ΔE (V)***
THCpSi	***0.295***	***0.110***	***239***	***158***	***0.185***
TCpSi	***0.270***	***0.150***	***262***	***584***	***0.120***
PFApSi	***0.260***	***0.140***	***310***	***295***	***0.120***

Biofilm characterization

Protocol optimization: To understand the pattern of growth of bacteria related to incubation time, *S. epidermis biofilms* were grown on 96 well plates and incubated for different time lengths (24, 48 and 72 h). Crystal violet assays were carried out to compare biomass quantifications for the different time points. Table 2 summarizes the results from this study. The 24 h time point performed the best with a slightly higher optical density, taking less time to complete the experiment and corresponding with the log phase of bacterial growth which is of interest for biofilm studies [11].

Table 2: Optical density of S. epidermis biofilms cultured for 24, 48 and 72 h.

Culture time	24 h		48 h		72 h	
Experimental group	*Control*	*Sample*	*Control*	*Sample*	*Control*	*Sample*
Average OD ± SD	0.11 ± 0.03	3.68 ± 0.05	0.06 ± 0.00	3.54 ± 0.04	0.12 ± 0.08	3.36 ± 0.22

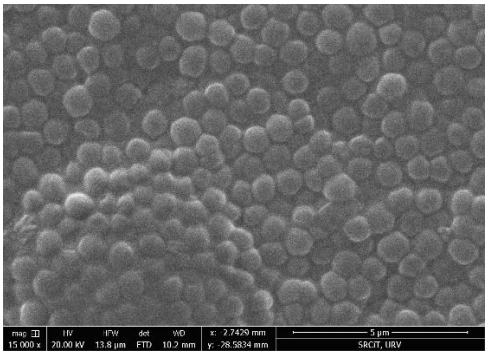

Figure 3: SEM image of the S. epidermis biofilm grown on a TCpSi substrate. Image taken at x15,000 magnification with a secondary electron detector. Spherical S. epidermis cells are visible. Average size of cell is 814 nm ± 41 nm, which is in the normal size range of S. epidermis found in the literature [24]**.**

SEM images confirm a monospecies biofilm is grown using the culturing protocols described above. The culturing protocols are not only successful in growing a biofilm but also preventing contamination of the culture with other microbes (e.g. other bacteria species or yeast). The spherical shape shown in Figure 3 and the average size calculated from this image (814 nm ± 41) agree with those previously reported for *S. epidermis* [24].

Upon optimization of the biofilm growth conditions of *S. epidermis* on well plates, the same conditions were applied to grow *S. epidermis* biofilms on THCpSi, TCpSi and PFApSi samples (at 37°C for 24 h). Both live and dead bacteria were stained using LIVE/DEAD™ BacLight™ and captured via separate laser excitations. The images were merged using ImageJ software and the intensity of fluorescence was measured. Merged images are shown in Figure 4 and the intensity results are shown in Table 3. Sample groups were cultured as described at the Materials and methods section, control groups were incubated at 37°C for 24 h with sterile media only.

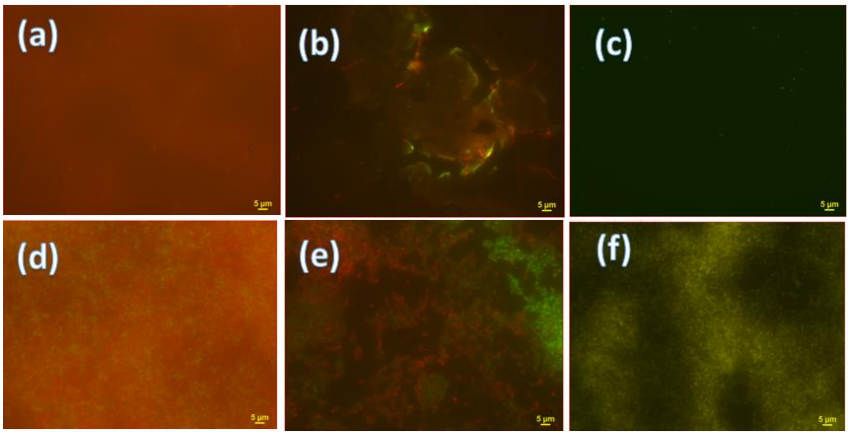

Figure 4: Fluorescent microscope images. (a), (b) and (c) are control groups for THCpSi, PFApSi and TCpSi, respectively. (d), (e) and (f) are the sample group for THCpSi, PFApSi and TCpSi, respectively. Dead bacteria are stained red and live bacteria are green. Images are merged using ImageJ software.

Table 3: Fluorescence intensity measured from the images depicted in Figure 4 using ImageJ software. The difference of fluorescence intensity between samples and controls has been normalized as follows: $\Delta FI = ((FI_{sample}-FI_{control})/FI_{control}) \times 100$, where ΔFI is the normalized fluorescence intensity difference between samples and controls, and FI_{sample} and $FI_{control}$ are the average fluorescence intensity values for samples and controls, respectively.

Type of carbon-stabilized pSi	FI_{sample}	$FI_{control}$	ΔFI
THCpSi	146	108	35%
PFApSi	63	50	26%
TCpSi	54	14	286%

Fluorescence intensity values were calculated by combining the intensity from both SYTO 9 (Green) and propidium Iodide (Red) stains which stained live and dead bacteria, respectively. Although TCpSi shows the lowest fluorescence intensity (FI) in the sample group when compared to THCpSi and PFApSi, this is the only substrate with relatively low values of FI in the control group. Therefore, according to characterization of the biofilm based on the fluorescence intensity emitted, , these results indicate that TCpSi potentially offer the best substrate for biofilm growth. However, the high FI values in all control groups need to be addressed.

Based on these preliminary results, further optimization of the culturing and staining protocols is needed, but also the interactions between the stains used and the surface of pSi needs to be investigated in order to determine if any non-specific adsorption is occurring. To this purpose, FTIR analysis which is later discussed investigates the bonds formed between dyes and pSi samples to point out the strategies that might help to minimize non-specific adsorption of the dyes on THCpSi, TCpSi and PFApSi.

Crystal violet staining experiments similarly showed increased optical density in TCpSi, THCpSi and PFApSi control groups. The results are summarized in Table 5.

Table 5. Optical density (OD) readings measured at 570 nm. Average OD values and associated standard deviations (SD) obtained from S. epidermis grown on THCpSi, TCpSi and PFApSi substrates. The difference of OD between samples and controls has been normalized as follows: $\Delta OD = ((OD_{sample}-OD_{control})/OD_{control}) \times 100$, where ΔOD is the normalized OD difference between samples and controls, and OD_{sample} and $OD_{control}$ are the average fluorescence intensity values for samples and controls, respectively.

Type of carbon-stabilized pSi and experimental group	Average OD ± SD	ΔOD
TCpSi control group	2.14 ± 0.45	56%
TCpSi sample group	3.35 ± 0.02	
THCpSi control group	2.00 ± 0.17	93%
THCpSi sample group	3.86 ± 0.04	
PFApSi control group	2.24 ± 0.50	49%
PFApSi sample group	3.33 ± 0.14	

THCpSi performs better in these experiments with both the highest optical density (OD) and ΔOD when comparing the control groups to the experimental groups. The higher ΔOD, almost two-fold that of TCpSi and PFApSi, indicates a higher biomass. This agrees with the high FI values shown previously by THCpSi when compared to TCpSi and PFApSi. Thus, THCpSi substrates are more conducive to bacterial growth and biofilm formation. As with the FI measurements, the control groups exhibit relatively high OD which needs to be investigated further to suppress or minimize potential non-specific adsorptions of dyes.

FTIR analysis of dye- pSi surface interactions

To investigate the high FI and OD values observed in the control groups, FTIR was carried out to identify any non-specific adsorption of the dye on each type of carbon-stabilized pSi.

For THCpSi and TCpSi unique peaks were found when exposed to crystal violet, propidium iodide and SYTO 9. Whereas for PFApSi unique peaks were only observed when exposed to crystal violet. A full list of the unique peaks for all samples can be found in Table S1 in the supplementary section. Therefore the method of carbon stabilization influences the

surface chemistry of the resulting pSi substrate, further investigation is needed into what reactive groups are interacting with the specific dyes in order to fully evaluate the suitability of each dye for use with each pSi substrate.

Electrochemical analysis

Electrochemical measurements were taken first on bare THCpSi as higher values of both bacterial biomass and viability were observed on this substrate when compared to TCpSi and PFApSi.. *S. epidermis* biofilms were then grown on the TCHpSi surface by incubation in TSB media for 24 h at 37°C. Control groups were incubated in sterile TSB media 24 h at 37°C. Table 2 shows the key parameters from cyclic voltammetry results for the control and experimental groups, performed in a 2 mM measuring solution.

Table 6: Electrochemical analysis. Epa, Epc, Ipa, Ipc, and ΔE values from CV results using THCpSi as working electrode, and a 2 mM ferrocyanide and ferricyanide in 10 mM PBS measuring solution. Results are shown for the control and experimental groups both before and after incubation with TSB media and bacteria in TSB media, respectively.

SAMPLES	*Epa (V)*	*Epc (V)*	*Ipa (μA)*	*Ipc (μA)*	*ΔE (V)*
Control: Before TSB media incubation	***0.295***	***0.110***	***239***	***158***	***0.185***
Control: After TSB media incubation	***0.295***	***0.105***	***230***	***185***	***0.190***
Experimental: Before bacterial growth	***0.255***	***0.135***	***218***	***208***	***0.120***
Experimental: After bacterial growth	***0.285***	***0.130***	***120***	***128***	***0.155***

Table 6 shows the drastic decrease in Ipa and Ipc values after the biofilm was grown on the substrate is a promising result indicating that CV measurements can be used to detect the presence of biofilm on the surface of THCpSi. This is supported by the absence of such decrease in the control sample after media incubation. In addition, the ΔE of 35 mV increase for the sensor, compared to the 5 mV increase for the control, also supports the presence of the biofilm on THCpSi hindering the electron transfer on the pSi electrode surface.

Conclusion

Here three types of carbon-stabilized pSi, i.e. THCpSi, TCpSi and PFApSi, have been successfully fabricated to be used both as substrates for bacterial biofilm growth and electrodes. Other ways to stabilize the pSi post etching, such as thermal oxidation, can be further considered, as well as various functionalization strategies to tune their surface chemistry. In addition, various biological and polymer compounds can also be introduced onto the surfaces of the pSi electrodes. Such versatility paves the way towards the development of new sensing platforms able to monitor in real time the growth of bacterial biofilms, what can be used to quickly identify the antibiotic resistance of particular bacterial strains.

The preliminary results shown herein underpin the successful growth of *S. epidermis* on the three types of carbon-stabilized pSi substrates tested. Optical characterization using various dyes confirmed the growth of the biofilm. However, results showed significant non-specific adsorption of the dyes on all pSi samples. Therefore, further investigation on why dyes adsorb on each substrate, to later design strategies to minimize such effect are required. X-ray diffraction is a potential method that would complement the already completed FTIR analysis by giving more information on the chemical composition and structures found on the surface.

Electrochemical analysis shows promising results for the detection of the biofilm grown on the surface. Characterization of THCpSi substrates before and after biofilm growth via cyclic voltammetry in a 2 mM ferrocyanide and ferricyanide solution in 10 mM PBS buffer underpinned the presence of the biofilm through a significant decrease in both Ipa and Ipc

and increase in ΔE. This agrees with our hypothesis that the presence of the biofilm over the electrode surface strongly hinders the electron transfer. THCpSi was chosen over TCpSi and PFApSi as higher bacterial biomass and viability was observed on the THCpSi substrates.

The next steps involve studying the effects of different pSi morphologies and surface functionalizations on biofilm growth.

Given the economic and patient impact of biofilms in the medical field it is understandable to focus on developing solutions that are relevant to a clinical setting. However, there are many more industries that a biofilm sensor would prove to a massive boon for. Developing a sensor that can non-destructively detect and real-time monitor bacterial biofilm growth is a very worthwhile endeavour with a wide market.

References

[1] P. Gupta, S. Sarkar, B. Das, S. Bhattacharjee, and P. Tribedi, "Biofilm, pathogenesis and prevention—a journey to break the wall: a review," *Arch Microbiol*, vol. 198, no. 1, pp. 1–15, Jan. 2016, doi: 10.1007/s00203-015-1148-6.

[2] L. Bircher, C. Schwab, A. Geirnaert, A. Greppi, and C. Lacroix, "Planktonic and Sessile Artificial Colonic Microbiota Harbor Distinct Composition and Reestablish Differently upon Frozen and Freeze-Dried Long-Term Storage," *mSystems*, vol. 5, no. 1, Feb. 2020, doi: 10.1128/mSystems.00521-19.

[3] C. Beloin, A. Roux, and J.-M. Ghigo, "Escherichia coli Biofilms," 2008, pp. 249–289. doi: 10.1007/978-3-540-75418-3_12.

[4] J. Haiko and B. Westerlund-Wikström, "The role of the bacterial flagellum in adhesion and virulence," *Biology*, vol. 2, no. 4. MDPI AG, pp. 1242–1267, Oct. 25, 2013. doi: 10.3390/biology2041242.

[5] L. A. Pratt and R. Kolter, "Genetic analysis of *Escherichia coli* biofilm formation: roles of flagella, motility, chemotaxis and type I pili," *Mol Microbiol*, vol. 30, no. 2, pp. 285–293, Oct. 1998, doi: 10.1046/j.1365-2958.1998.01061.x.

[6] G. Sharma *et al.*, "*Escherichia coli* biofilm: development and therapeutic strategies," *J Appl Microbiol*, vol. 121, no. 2, pp. 309–319, Aug. 2016, doi: 10.1111/jam.13078.

[7] C. M. Müller, A. Åberg, J. Straseviçiene, L. Emődy, B. E. Uhlin, and C. Balsalobre, "Type 1 Fimbriae, a Colonization Factor of Uropathogenic Escherichia coli, Are Controlled by the Metabolic Sensor CRP-cAMP," *PLoS Pathog*, vol. 5, no. 2, p. e1000303, Feb. 2009, doi: 10.1371/journal.ppat.1000303.

[8] A. L. S. dos Santos *et al.*, "What are the advantages of living in a community? A microbial biofilm perspective!," *Mem Inst Oswaldo Cruz*, vol. 113, no. 9, Jul. 2018, doi: 10.1590/0074-02760180212.

[9] P. Gupta, S. Sarkar, B. Das, S. Bhattacharjee, and P. Tribedi, "Biofilm, pathogenesis and prevention—a journey to break the wall: a review," *Arch Microbiol*, vol. 198, no. 1, pp. 1–15, Jan. 2016, doi: 10.1007/s00203-015-1148-6.

[10] M. E. Davey and G. A. O'toole, "Microbial Biofilms: from Ecology to Molecular Genetics," *Microbiology and Molecular Biology Reviews*, vol. 64, no. 4, pp. 847–867, Dec. 2000, doi: 10.1128/MMBR.64.4.847-867.2000.

[11] S. Becerro, J. Paredes, M. Mujika, E. Perez Lorenzo, and S. Arana, "Electrochemical Real-Time Analysis of Bacterial Biofilm Adhesion and Development by Means of Thin-Film Biosensors," *IEEE Sens J*, vol. 16, no. 7, pp. 1856–1864, Apr. 2016, doi: 10.1109/JSEN.2015.2504495.

[12] F. M. Carvalho, R. Teixeira-Santos, F. J. M. Mergulhão, and L. C. Gomes, "The Use of Probiotics to Fight Biofilms in Medical Devices: A Systematic Review and Meta-Analysis," *Microorganisms*, vol. 9, no. 1, p. 27, Dec. 2020, doi: 10.3390/microorganisms9010027.

[13] A. Reisner *et al.*, "Type 1 Fimbriae Contribute to Catheter-Associated Urinary Tract Infections Caused by Escherichia coli," *J Bacteriol*, vol. 196, no. 5, pp. 931–939, Mar. 2014, doi: 10.1128/JB.00985-13.

[14] P. Pronovost *et al.*, "An Intervention to Decrease Catheter-Related Bloodstream Infections in the ICU," *New England Journal of Medicine*, vol. 355, no. 26, pp. 2725–2732, Dec. 2006, doi: 10.1056/NEJMoa061115.

[15] H.-C. Flemming, J. Wingender, U. Szewzyk, P. Steinberg, S. A. Rice, and S. Kjelleberg, "Biofilms: an emergent form of bacterial life," *Nat Rev Microbiol*, vol. 14, no. 9, pp. 563–575, Sep. 2016, doi: 10.1038/nrmicro.2016.94.

[16] C. Deirmengian, K. Kardos, P. Kilmartin, S. Gulati, P. Citrano, and R. E. Booth, "The Alpha-defensin Test for Periprosthetic Joint Infection Responds to a Wide Spectrum of Organisms," *Clin Orthop Relat Res*, vol. 473, no. 7, pp. 2229–2235, Jul. 2015, doi: 10.1007/s11999-015-4152-x.

[17] Y. Xu, Y. Dhaouadi, P. Stoodley, and D. Ren, "Sensing the unreachable: challenges and opportunities in biofilm detection," *Curr Opin Biotechnol*, vol. 64, pp. 79–84, Aug. 2020, doi: 10.1016/j.copbio.2019.10.009.

[18] C. Q. Nguyen *et al.*, "Longitudinal Monitoring of Biofilm Formation via Robust Surface-Enhanced Raman Scattering Quantification of *Pseudomonas aeruginosa* -Produced Metabolites," *ACS Appl Mater Interfaces*, vol. 10, no. 15, pp. 12364–12373, Apr. 2018, doi: 10.1021/acsami.7b18592.

[19] N. F. Azevedo, M. J. Vieira, and C. W. Keevil, "Establishment of a continuous model system to study Helicobacter pylori survival in potable water biofilms," *Water Science and Technology*, vol. 47, no. 5, pp. 155–160, Mar. 2003, doi: 10.2166/wst.2003.0307.

[20] L. Liu *et al.*, "Monitoring of bacteria biofilms forming process by in-situ impedimetric biosensor chip," *Biosens Bioelectron*, vol. 112, pp. 86–92, Jul. 2018, doi: 10.1016/j.bios.2018.04.019.

[21] D. L. Bellin *et al.*, "Integrated circuit-based electrochemical sensor for spatially resolved detection of redox-active metabolites in biofilms," *Nat Commun*, vol. 5, no. 1, p. 3256, May 2014, doi: 10.1038/ncomms4256.

[22] M. Hosseini, S. Zaeemi Baravati, Z. Jokar, and S. Ganji Chermahin, "Clinical characteristics of Staphylococcus epidermidis: a systematic review Klinische Charakterisierung von Staphylococcus epidermidis: ein systematisches Review Staphylokokken sind ein Cluster Gram-positiver unbeweglicher nicht Sporen-

bildender fakultativ anaerober Kokkenbakterien, die in die zwei Hauptgruppen Coagulase-positiv and Coagulase-negativ unterteilt wer."

[23] K. Guo *et al.*, "Porous Silicon Nanostructures as Effective Faradaic Electrochemical Sensing Platforms," *Adv Funct Mater*, vol. 29, no. 24, p. 1809206, Jun. 2019, doi: 10.1002/adfm.201809206.

[24] Yuqing Li and Xuedong Zhou, Eds., *Atlas of Oral Microbiology From Healthy Microflora to Disease*, 1st ed. Elsevier Inc.

Supplementary Information

Electrochemical characterization of THCpSi, TCpSi and PFApSi

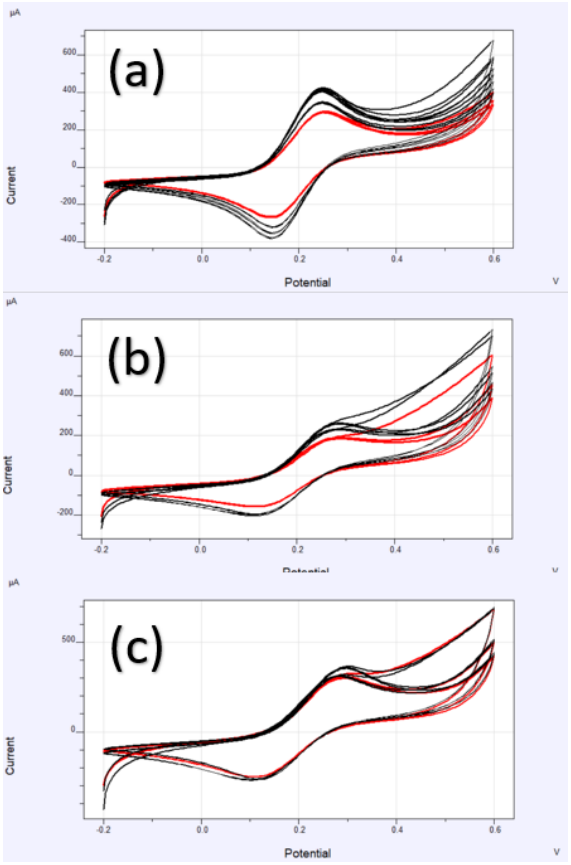

Figure S1. Cyclic voltammograms measured in a ferrocyanide and ferricyanide [$Fe(CN_6)]^{3-/4-}$] prepared in 10 mM PBS buffer solution using THCpSi. (a) before and (b) after biofilm growth, and (c) are controls incubated in sterile TSB media.

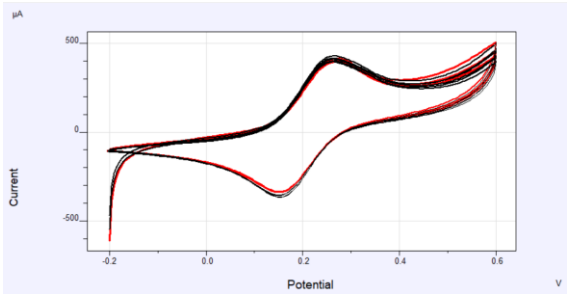

Figure S2. Cyclic voltammograms measured in a ferrocyanide and ferricyanide [$Fe(CN_6)]^{3-/4-}$] prepared in 10 mM PBS buffer solution using bare TCpSi.

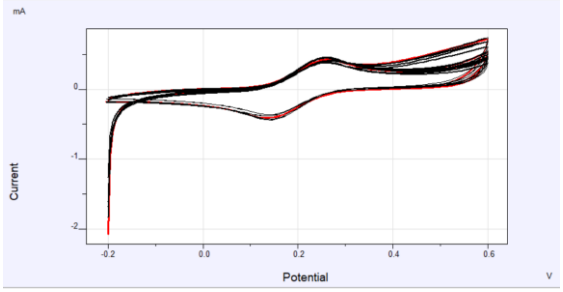

Figure S3. Cyclic voltammograms measured in ferrocyanide and ferricyanide [$Fe(CN_6)]^{3-/4-}$] prepared in 10 mM PBS buffer solution using bare PFApSi.

FTIR analysis: To study non-specific adsorption of dyes on carbon-stabilized pSi

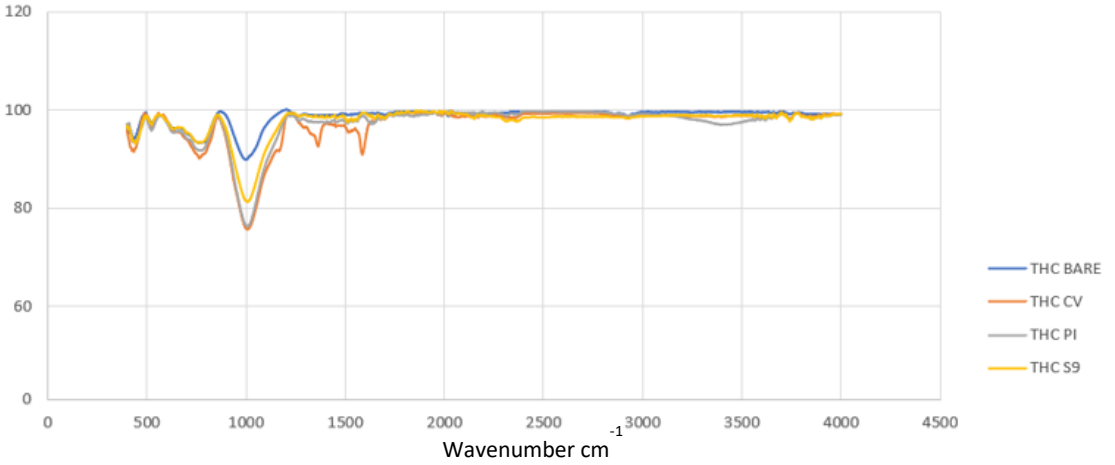

Figure S4: FTIR analysis of dye interactions and THCpSi. Legend: THC bare is bare THCpSi, and THC CV, THC PI and THC S9 are THCpSi stained with crystal violet, propidium iodide and SYTO 9, respectively.

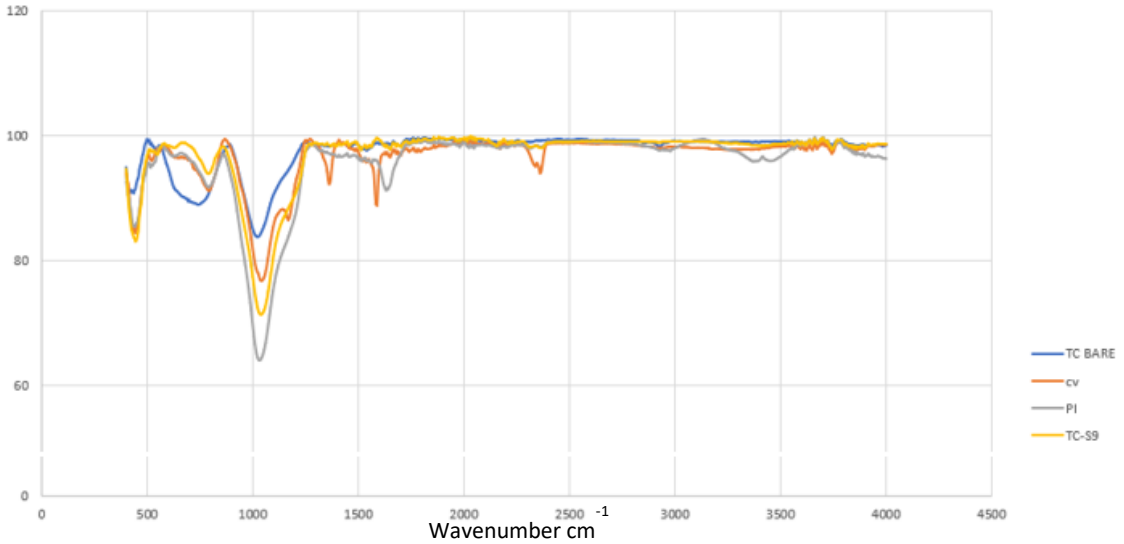

Figure S5: FTIR analysis of dye interactions and TCpSi. Legend: TC bare is bare TCpSi, and TC CV, TC PI and TC S9 are TCpSi stained with crystal violet, propidium iodide and SYTO 9, respectively.

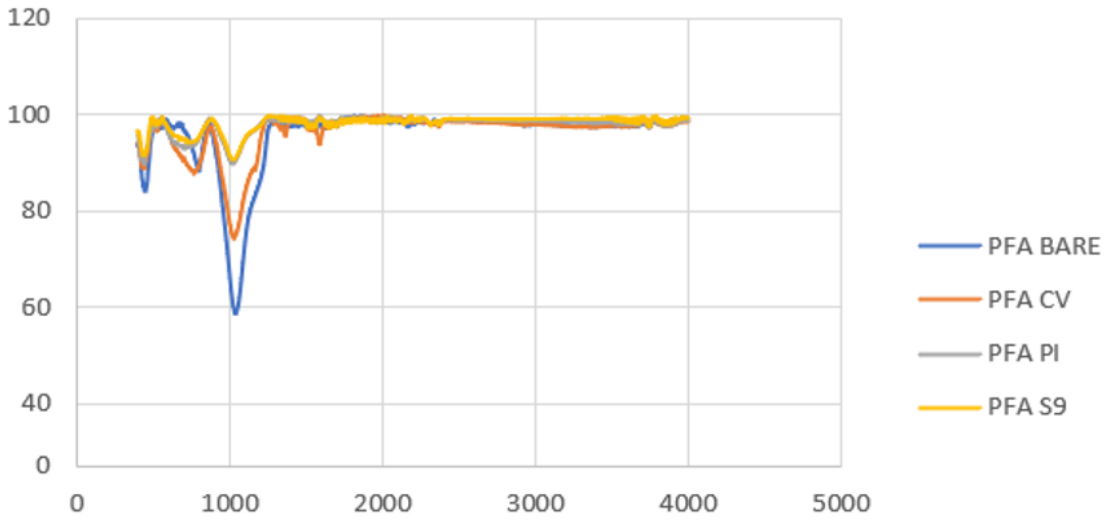

Figure S6: FTIR analysis of dye interactions and PFApSi. Legend: PFA bare is bare PFApSi, and PFA CV, PFA PI and PFA S9 are PFApSi stained with crystal violet, propidium iodide and SYTO 9, respectively.

Table S1: FTIR bands for TCpSi, THCpSi and PFApSi exposed to various dyes.

Type of carbon-stabilized pSi	**Crystal violet**	**Propidium iodide**	**SYTO 9**
TCpSi	2361.41 cm^{-1} (O=C=O carbon dioxide) 1586.16 cm-1 (N-O) 1361.5 cm-1 (O-H) (phenol)	3372.89 cm-1 (N-H) 2977.55 cm-1 (N-H OR C-H) 2369.12 cm-1 (O=C=O Carbon dioxide) 2316.09 cm-1 (O=C=O Carbon dioxide) 1631.48 cm-1 (N-H)	2366.23 cm-1 (O=C=O carbon dioxide) 2304.52 cm-1 (O=C=O carbon dioxide) 2152.17 cm-1 (C=C=O Ketone)
THCpSi	1586.16 cm-1 (N-O nitro compound) 1362.46 cm-1 (N-O nitro compound)	3397.96 cm-1 (N-H aliphatic primary amine) 1630.52 cm-1 (N-H amine)	2368.16 cm-1 (O=C=O carbon dioxide) 2312.23 cm-1 (O=C=O carbon dioxide)
PFApSi	1588.09 cm-1 (N-H amine) 1364.39 cm-1 (O-H phenol)	N/A	N/A